

*INVESTIGATION OF THE DE HAAS-VAN ALPHEN EFFECT IN BISMUTH AT ULTRA-LOW TEMPERATURES*

N. B. BRANDT, T. F. DOLGOLENKO, and N. N. STUPOCHENKO

Moscow State University

Submitted to JETP editor April 24, 1963

J. Exptl. Theoret. Phys. (U.S.S.R.) **45**, 1319-1335 (November, 1963)

Quantum oscillations of the magnetic susceptibility of bismuth for various crystallographic orientations of the samples in a magnetic field at temperatures between 0.08 and 0.12°K are investigated in detail. The shape of the Fermi surface in bismuth is examined on the basis of the results obtained.

## INTRODUCTION

INVESTIGATIONS of quantum oscillations of the magnetic susceptibility of bismuth at ultra-low temperatures<sup>[1-3]</sup>, have disclosed new, heretofore unobserved, high-frequency oscillations connected with the hole part of the Fermi surface; it was established that the latter can be approximated, in first approximation, by an ellipsoid of revolution prolate along the trigonal axis. At the same time, however, many singularities were observed, the nature of which cannot be ascertained for the lack of sufficiently strong magnetic fields and the inadequacy of the measurement procedure. Since the sensitivity of the procedure was appreciably improved by us and the range of magnetic fields increased, it seemed of interest to investigate this group of oscillations in greater detail.

In addition, it was of interest to investigate in greater detail the oscillations connected with the electronic part of the Fermi surface. We recall that according to the Jones-Shoenberg model, the electronic part of the Fermi surface consists of three strongly elongated triaxial ellipsoids, oriented in quasi-momentum space in such a way, that the shortest axes of the ellipsoids coincide with the binary axes while the longest axes are inclined to a plane perpendicular to the trigonal axis by an angle  $\xi \approx 6^\circ$ . The ellipsoids go over into one another by rotation through 120° about the trigonal axis.

In numerous investigations of the oscillations of the magnetic susceptibility<sup>[4-7]</sup>, of the electric resistivity, the Hall emf<sup>[8-16]</sup>, and the surface impedance at microwave frequency<sup>[17]</sup>, the only oscillations observed correspond to the minimal and intermediate ellipsoid sections. The oscillations connected with the largest principal sections of

the ellipsoids were apparently not observed because of their small amplitude. Since the high-frequency oscillation amplitude connected with the large areas of the extremal Fermi sections increases strongly with decreasing temperature, we can hope that these oscillations will become observable in measurements in the region of ultra-low temperatures.

In the present paper we present the results of detailed investigations of quantum oscillations of the magnetic susceptibility in bismuth for different orientations of the crystal in a magnetic field at 0.08-1.12°K.

## MEASUREMENT PROCEDURE, SAMPLES

The anisotropy  $\Delta\chi$  of the magnetic susceptibility was measured in a homogeneous magnetic field of intensity up to 15 kOe, using a magnetic torsion balance intended for measurements at ultra-low frequencies<sup>[2]</sup>. The balance was equipped with a servomechanism that permitted the measurements to be carried out at a fixed specimen orientation, with the magnetic field turned on either gradually or in steps<sup>[8]</sup>. The elasticity of the suspension rod, and the displacement of the indicator relative to the differential photoresistance that produced the required compensating torque, cause the sample to deviate not more than 2' from its fixed position.

The magnetic field intensity was determined by a ballistic method and monitored against the known value of the anisotropy of the magnetic susceptibility of bismuth at room temperature; it was also determined by the paramagnetic resonance method using the IMI-2 instrument. During the measurements, the field was determined from the value of the current in the magnet, which was measured with a potentiometer.

A temperature of approximately 0.08°K was produced by adiabatic magnetization of a pellet of iron ammonium alum, and was measured by determining the susceptibility. The measurement was made while the specimen was heated from 0.08 to 0.12°K.

The samples were made of 99.998% pure Hilger bismuth, purified by 20-fold recrystallization in vacuum, and of bismuth from the Kharkov Physico-technical Institute<sup>1)</sup>. The latter contained, according to qualitative spectral analysis, traces of Mn, Al, Mg, Cu, Fe, Si, Pb, and Ag. In both types of bismuth, the electric resistance changed by 300–400 times on cooling from 300 to 4.2°K.

Single crystals in the form of cylinders approximately 4 mm in diameter and 5–7 mm long were grown in Pyrex ampoules by the method of P. L. Kapitza<sup>[19]</sup> in such a way that their trigonal and geometrical axis were parallel. The direction of the binary axes was determined with a goniometer accurate to ±0.3°. The samples were annealed in a helium atmosphere at 240 to 140°C in succession for five and 10 days. The samples were mounted in holders of three types: the first type<sup>[2]</sup> was used for measurements with the magnetic field oriented in the planes perpendicular to the binary axis and the bisector, while the two other types (Fig. 1) were used for measurements in the basal plane and for arbitrary sample orientation.

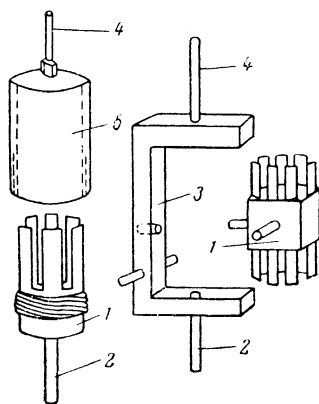


FIG. 1. Holders for samples: 1 – copper band, 2 – cold pipe, 3 – copper bracket, 4 – rod of suspension system, 5 – Plexiglas cup.

## MEASUREMENT RESULTS

The measurement was carried out for three main orientations of the crystal relative to the suspension axis of the torsion balance (suspension axis perpendicular to the magnetic field):

1. The trigonal axis perpendicular to and the binary axis parallel to the suspension axis ( $\psi$  —

angle between the direction of the trigonal axis and the magnetic field).

II. The trigonal and binary axes perpendicular to the suspension axis ( $\psi$  — angle between the direction of the trigonal axis and the magnetic field).

III. Trigonal axis parallel to the suspension axis ( $\psi$  — angle between the binary axis and the magnetic field).

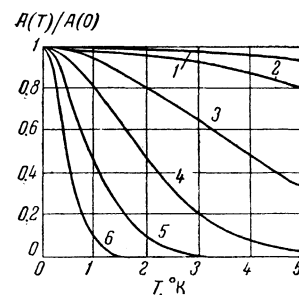
At ultra-low temperatures, the curves of the magnetic moment  $M$  against  $1/H$ , unlike the curves plotted at helium temperatures, become much more complicated. It must be borne in mind in the analysis of the data that this complication can be caused by the following factors.

1. Deviation of the curve from sinusoidal because of the increased harmonic content. For a quadratic dispersion law, the oscillating part of the magnetic susceptibility, connected with the section  $S_i$  of the Fermi surface, is given by the formula<sup>[4,5]</sup>

$$\Delta\chi = \frac{A}{\rho} \frac{a_i}{T^{1/2}} \left( \frac{2\pi^2 kT}{\beta_i H} \right)^{3/2} \times \sum_{l=1}^{\infty} (-1)^l \sin \left( \frac{2\pi p E_0}{\beta_i H} - \frac{\pi}{4} \right) \exp \left( \frac{-3\pi^2 l k x_i}{\beta_i H} \right) \times 2 l^{-1/2} \sinh \left( \frac{2\pi^2 l k T}{\beta_i H} \right)^{-1}, \quad (1)$$

where  $\beta_i = (eh/c)(dS/dE)^{-1}$  (double the effective Bohr magneton),  $k$  — Boltzmann's constant,  $\rho$  — density,  $A$  — constant,  $a_i$  — function dependent on the orientation of the magnetic field  $H$ , and  $x_i$  — Dingle factor. Figure 2 shows the temperature de-

FIG. 2. Temperature dependence of the relative variation of the amplitude  $A$  of the harmonics corresponding to the sections  $S_1$  (curves 1, 2, and 3—1 = 1, 2, and 5, respectively) and  $10S_1$  (curves 4, 5, and 6—1 = 1, 2, and 4).



pendence of the harmonic amplitudes corresponding to the minimum section of the Fermi surface ellipsoid,  $S_1$ , and the section of area  $10S_1$ . It is seen from the figure that the amplitudes of the fundamental (first) harmonic and also the amplitudes of the second and fifth harmonics corresponding to the section  $S_1$  vary little on going to ultra-low temperatures. On the contrary, the amplitude of the first harmonic is much larger for the section  $10S_1$  and an even greater increase is observed in the amplitudes of the second and subsequent har-

<sup>1)</sup>We take the opportunity to thank B. N. Aleksandrov for graciously supplying the bismuth.

monics. In this connection, we can expect the harmonics to become more clearly pronounced for the large sections and to increase only slightly for the small Fermi-surface sections.

2. Strong increase in the amplitude of the oscillations, due to the large sections of the electronic part of the Fermi surface, not observed in the region of helium temperatures.

3. Sharp increase in the amplitude of the oscillations, due to the hole part of the Fermi surface.

4. Several singularities of the high-frequency oscillations, which are manifest at definite orientations of the magnetic field.

Characteristic examples of the dependence of  $M$  on  $1/H$  are shown in Fig. 3. It is seen from the figure that in most cases the curves are superpositions of several frequencies. A graphic method was used to separate the frequencies with sufficiently large difference, and in more complicated cases an approximate harmonic analysis was made with the aid of a Mader analyzer<sup>[20]</sup>.

Figures 4–6 show the angular dependence of the oscillation frequency (proportional to the areas of the extremal Fermi-surface intersections with the plane perpendicular to the direction of the magnetic field) for orientations I, II, and III. It is seen from Fig. 4 that the data obtained for different samples agree sufficiently well with one another, so that the results need not be connected with the purity of the specimens.

The oscillations observed at helium temperatures correspond to the sections of the curve a–b, b–c–d, and e–f on Fig. 4, sections a–b and c–d on Fig. 5, and the section a–b–c on Fig. 6. The oscillations observed at ultra low frequencies correspond to sections g–b, f–h, i–k–l, m–n, and i–o–l on Fig. 4, sections e–f, g–h, i–k, l–m–n on Fig. 5, and section a–e–c on Fig. 6. Let us consider the features of these oscillations for the different orientations.

**Orientation I.** The oscillations corresponding to section g–b on Fig. 4 are clearly observed at fields exceeding 5 kOe (see Fig. 3a curves for  $\psi = 10^\circ$  and  $\psi = 9^\circ$ ) and apparently pertain to the intersections between the electron "ellipsoid" and the plane passing through the binary axis of the reciprocal lattice. The amplitude of these oscillations decreases rapidly with decreasing angle and vanishes completely for  $\psi < 9^\circ$  (Fig. 3a, curve  $\psi = 8^\circ$ ). So rapid a decrease in the amplitude cannot be reconciled with the rate of vanishing [like  $\sin 2(\psi - 6^\circ)$ ] of the moment of the forces on approaching  $\psi = 6^\circ$ .

In the region of angles from 6 to  $8^\circ$  and near  $2^\circ$  in strong fields, oscillations with a frequency near

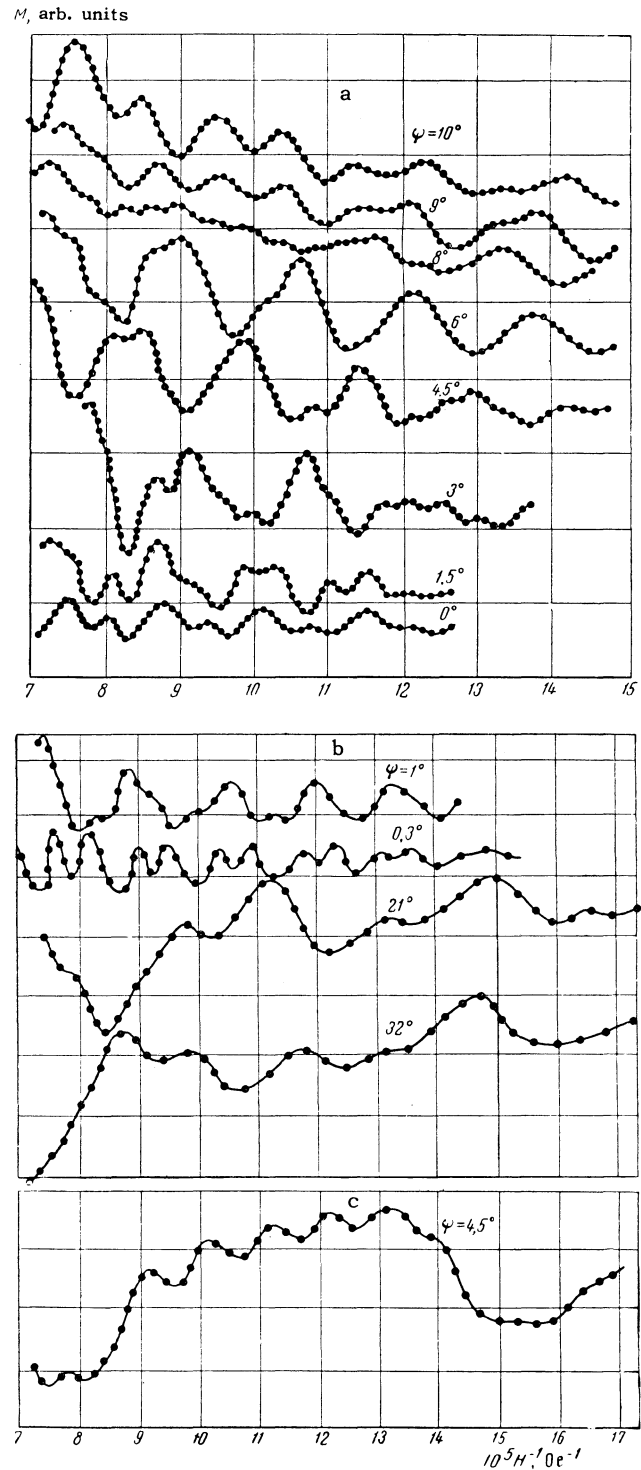


FIG. 3. Characteristic examples of the dependence of the magnetic moment  $M$  on  $1/H$  for bismuth: a—orientation I and  $T \approx 0.1^\circ\text{K}$ , b—orientation II and  $T \approx 0.1^\circ\text{K}$ , c—orientation III and  $T \approx 0.1^\circ\text{K}$ . (The numbers at the curves denotes the value of  $\psi$  in degrees.)

$26 \times 10^4 \text{ Oe}^{-1}$  appear (Fig. 3a). Simultaneously, oscillations of frequency  $(19-23) \times 10^4 \text{ Oe}^{-1}$  are distinctly observed in weak fields at  $1.5-3^\circ$ . In the interval  $3-7^\circ$  we observe oscillations with a

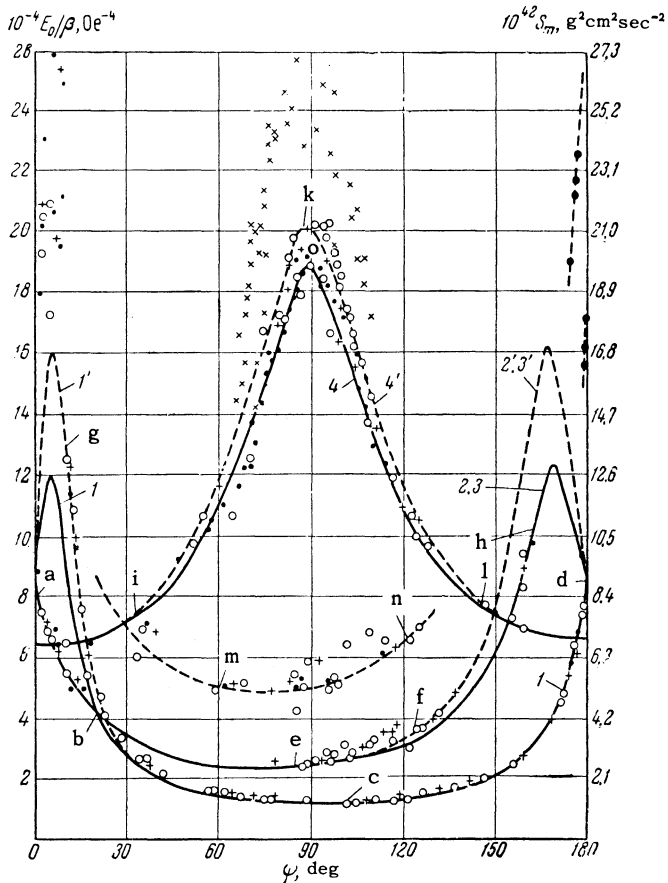


FIG. 4. Angular dependence of the oscillation frequency  $E_0/\beta$  and of the extremal values of  $S_m$  of the Fermi surface of bismuth for orientation I. The theoretical curves 1, 1'; 2, 2' and 3, 3' pertain to the three "ellipsoids" of the electronic part of the Fermi surface, while curves 4, 4' pertain to the hole part of the Fermi surface; points - experimental data;  $\circ$  - sample No. 1;  $\bullet$  - sample No. 2; + - sample No. 3.

frequency near  $20 \times 10^4 \text{ Oe}^{-1}$ . These oscillations have a complicated character, so that it is difficult to establish the angular dependence of their frequency (see, for example, Fig. 3a, curve  $\psi = 4.5^\circ$ ).

In the interval from  $6$  to  $1^\circ$  high frequency oscillations are observed, with an amplitude that decreases sharply on going away from  $\psi = 0^\circ$ . The angular dependence of the frequency of these oscillations is more clearly pronounced in the region of negative angles  $\psi$ , indicating that they are probably the second and third harmonics of the "ellipsoid" 1 (Fig. 4).

In the direct vicinity of zero ( $0 \pm 0.5^\circ$ ), the oscillations behave as if they were either superpositions of two nonsinusoidal curves of nearly equal frequency and amplitude, or else a superposition of the fundamental and doubled frequencies (Fig. 3a, curve  $\psi = 0$ ).

The amplitude of the high-frequency oscillations corresponding to f-h on Fig. 4, in the angle re-

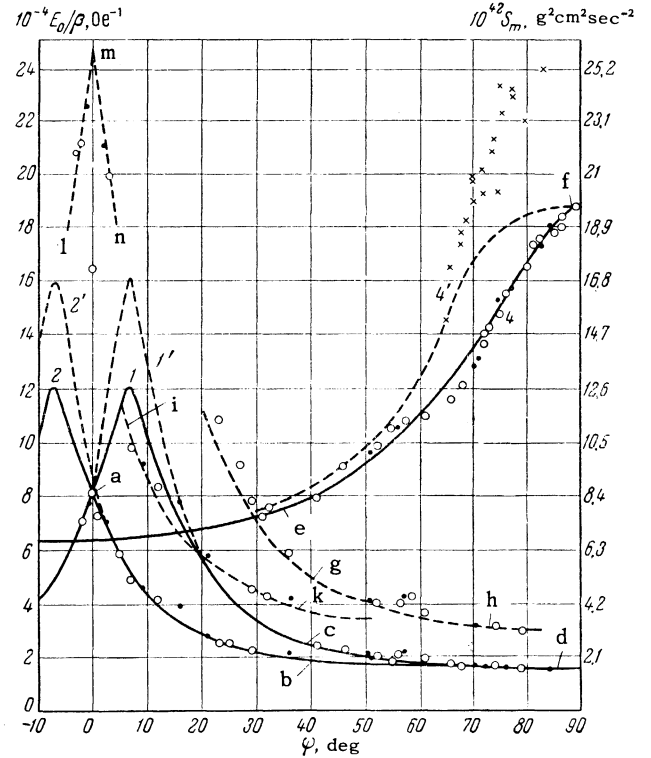


FIG. 5. Angular dependence of frequency of oscillations of  $E_0/\beta$  and extremal cross sections  $S_m$  of the Fermi surface of bismuth for orientation II. Curves 1, 1' and 2, 2' pertain to the two "ellipsoids" of the electronic part of the Fermi surface (no oscillations connected with the third ellipsoid were observed at this orientation), curves 4 and 4' pertain to the hole part of the Fermi surface. Points - experimental data;  $\circ$  - sample No. 1,  $\bullet$  - No. 2.

gion  $\psi = 120-160^\circ$ , decreases with increasing angle. Apparently these oscillations pertain to the coinciding sections of the two electron "ellipsoids" 2 and 3, which are turned in a complicated manner relative to the magnetic field. The oscillations in section e-f are apparently the third harmonic of the ellipsoid 1, while those on section m-n are harmonics of oscillations of "ellipsoids" 1, 2, and 3. On some curves of this type we observe clearly a transition from the low-frequency oscillations in weak fields to double the frequency in stronger fields. In addition, the angular dependence of their frequency exceeds in practice the angular dependence of the frequency of the fundamental oscillations.

High-frequency oscillations corresponding to the hole part of the Fermi surface are observed in the region of angles  $30-150^\circ$ . The curves i-k-l and i-o-l show the angular dependence of its extremal sections by planes passing respectively through the binary axis and the bisector of the reciprocal lattice.

Orientation II. The curves of Fig. 5 show the

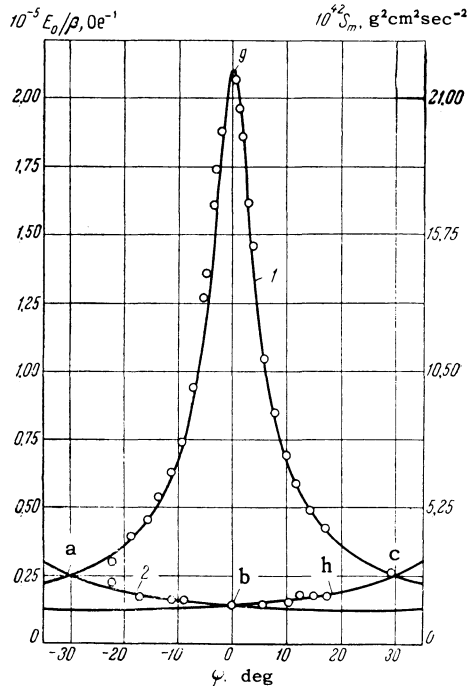


FIG. 6. Angular dependence of the oscillation frequency  $E_0/\beta$  and of the extremal cross sections  $S_m$  of the Fermi surface of bismuth for orientation III. Curves 1, 2, and 3 pertain to the three ellipsoids of the Fermi surface.

angular dependence of the extremal sections of equal-energy surfaces by the plane passing through the bisector of the reciprocal lattice. When  $\psi = 0^\circ$  this plane is located perpendicular to the trigonal axis, and the magnetic field is directed parallel to it.

The high frequency oscillations near  $0^\circ$  corresponding to sections  $l-m-n$  of the curve are probably, judging from the frequency and amplitude of the angular dependence, third harmonics of the fundamental oscillations (Fig. 3b, curve  $\psi = 1^\circ$ ). Sections  $i-k$  and  $g-h$  represent in all probability the second harmonic of the fundamental oscillations (Fig. 3b, curve  $\psi = 21^\circ$ ). The angular dependence of the amplitude of these oscillations is shown in Fig. 7.

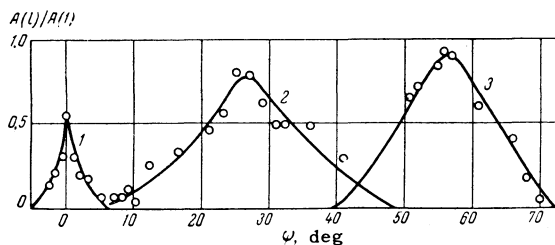


FIG. 7. Angular dependence of the relative amplitude of the harmonics at orientation II and  $T \approx 0.1^\circ\text{K}$ . Curve 1 corresponds to sections  $l-m-n$  of Fig. 5, curve 2—to section  $i-k$ , curve 3—to section  $g-h$ .

For values  $25^\circ \leq \psi \leq 32^\circ$  we observe clearly pronounced oscillations (Fig. 3b, curve  $\psi = 32^\circ$ ), whose amplitude is several times larger than the amplitude of the oscillations for the holes in this angle region and decreases sharply beyond the limits of this section. The nature of these oscillations is not clear.

Curve e-f pertains to the hole part of the Fermi surface. The  $M(1/H)$  curve plotted for orientation II and  $\psi \approx 0.3^\circ$  (Fig. 3b, curve  $\psi = 0.3^\circ$ ) recalls in its character the corresponding curve (Fig. 3a, curve  $\psi = 0$ ) plotted for orientation I.

**Orientation III.** Figure 6 shows the curves of the angular dependence of the extremal sections of the electron part of the Fermi surface with planes passing through the trigonal axis. The oscillations corresponding to section a-e-c pertain to the large sections of the electron equal-energy surface (Fig. 3,c). The hole surface does not appear at this orientation, since the associated moment of the forces is negligibly small.

**Features of high frequency oscillations.** The most interesting feature of the high frequency oscillations appears in the hole part of the Fermi surface, in the angle regions  $68^\circ < \psi < 78^\circ$  and  $102^\circ < \psi < 112^\circ$  (independently of the orientation I or II) and for the electron part of the Fermi surface in the narrower angle regions  $1^\circ < \psi < 4^\circ$  and  $-4^\circ < \psi < -1^\circ$  for orientation III. For the hole part of the Fermi surface, at  $68^\circ$  and  $112^\circ$ , the maxima of the fundamental frequency begins to split (Fig. 8). When the angles are changed towards  $\psi = 90^\circ$ , the magnitude of this effect increases. At the same time, the amplitude of the oscillations decreases. For  $\psi^* = 73^\circ$  and  $\psi^* = 107^\circ$  the splitting of the maxima reaches such a magnitude that the frequency of the oscillations doubles. With further change in angle, the character of the curves changes in reverse order. The angular dependence of the amplitude of the fundamental frequency and of the depth of the splitting is shown in Fig. 9. For the electronic part of the Fermi surface, the picture is analogous (Fig. 10).

Another singularity is manifest in the dependence of the oscillation frequency on the reciprocal field. It appears only for components of sufficiently high frequency and consists in the general case of having the frequency increase and decrease periodically with decreasing value of  $1/H$ . In most cases the period of this variation corresponds to the period of the fundamental low-frequency oscillations. The effect increases in strong magnetic fields, causing the frequency of the oscillations of highest frequency only to increase (for orientations

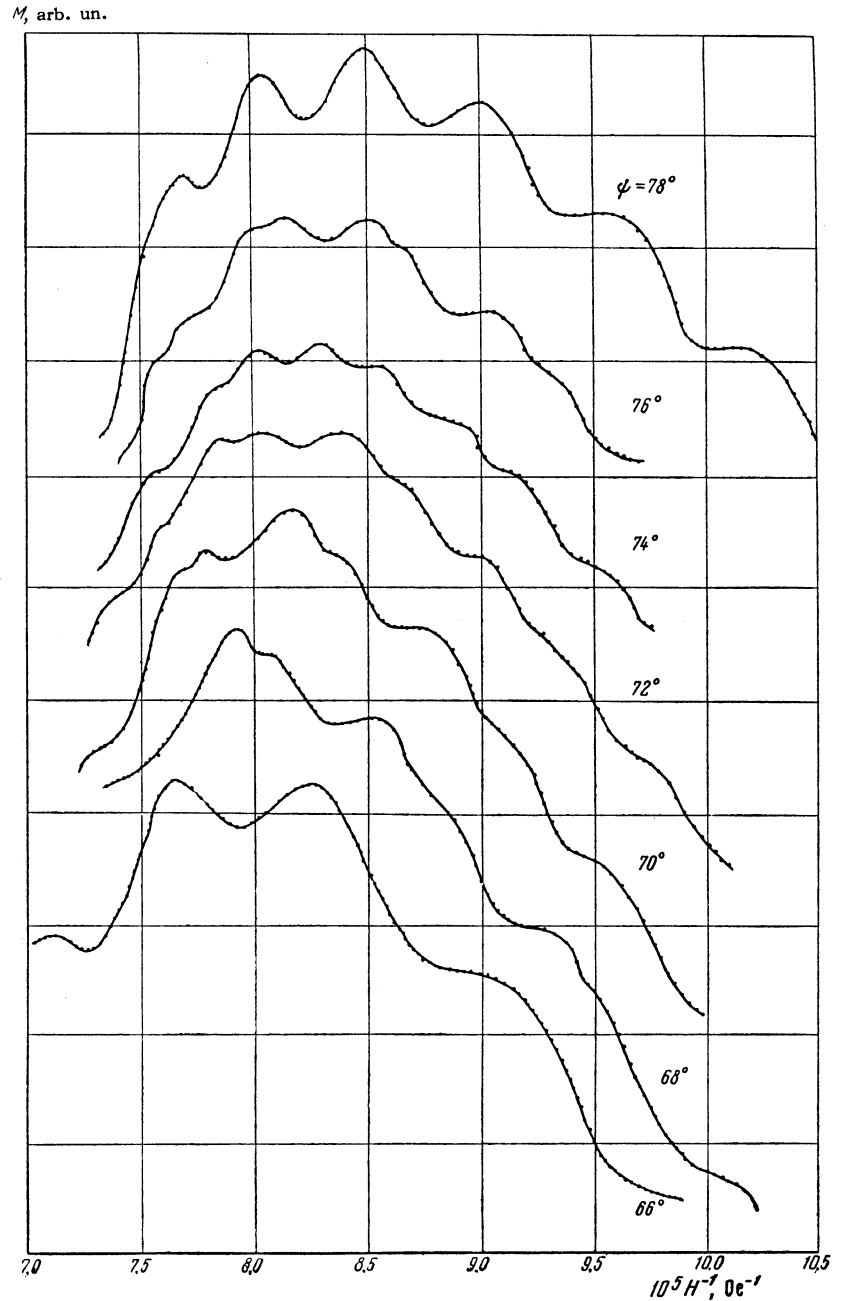


FIG. 8. Variation of the character of the oscillations connected with the hole part of the Fermi surface in angle region  $66^\circ \leq \psi \leq 78^\circ$ . Orientation II,  $T \approx 0.1^\circ\text{K}$ .

I and II) or only to decrease (for orientation III) with decreasing  $1/H$ , and making it very difficult to determine the frequency. We therefore took for the oscillations of Figs. 4–6 a frequency value averaged over several low-frequency periods, where possible in the weak-field region where the effect was small. The lying crosses on Figs. 4 and 5 denote the points corresponding to the higher frequency, determined for  $H > 11$  kOe. In the case of holes  $30\text{--}65^\circ$  and  $115\text{--}150^\circ$ , and in the case of electrons in the angle region  $\pm(8\text{--}30)^\circ$ , the oscillations plotted against  $1/H$  are practically equidistant in field from 3 to 14 kOe.

Temperature dependence of the oscillation am-

plitude. An investigation of the amplitude of the oscillations connected with the hole part of the Fermi surface at ultra low frequencies entails great difficulties since, on the one hand, the measurements are carried out during the course of the slow heating of the specimen and, on the other hand, owing to the Dingle factor, the amplitude of the oscillations practically ceases to depend on the temperature at sufficiently low temperatures. In this connection, the temperature dependence of the amplitude was investigated at  $1.6\text{--}2^\circ\text{K}$ . Since the amplitude of the high-frequency oscillations is quite low in this region, the measurements were made with very high sensitivity, after which the

M, arb. un.

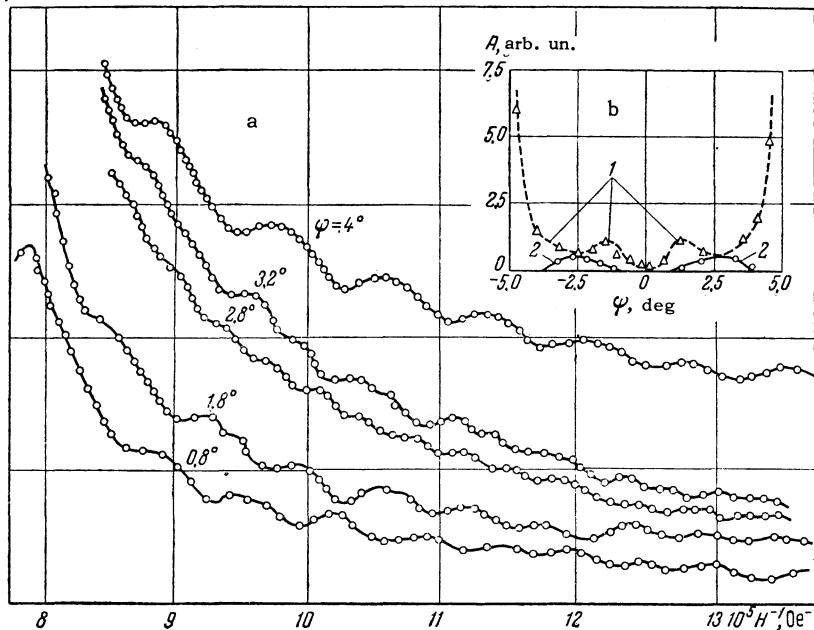


FIG. 10. a—variation of the character of the oscillations connected with the electron part of the Fermi surface in the angle region  $-5^\circ < \psi < 5^\circ$ ; orientation III,  $T \approx 0.1^\circ\text{K}$ . b—angle dependence of the oscillation amplitude (curve 1) and depth of splitting (curve 2) of "ellipsoid" 1 for orientation III;  $T \approx 0.1^\circ\text{K}$ ,  $H \approx 10$  kOe.

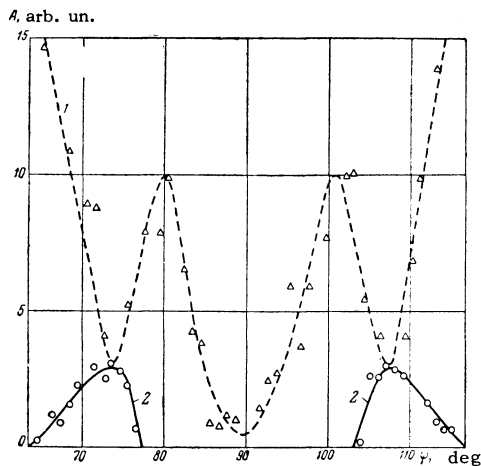


FIG. 9. Angular dependence of the amplitude of the oscillations (curve 1) and depth of splitting (curve 2) for the hole part of the Fermi surface at orientations I and II and  $T \approx 0.1^\circ\text{K}$  with  $H \approx 11$  kOe.

high-frequency component was separated graphically. Examples of the curves obtained in this manner for different angles  $\psi$  are shown in Fig. 11.

## DISCUSSION OF RESULTS

1. Hole part of the Fermi surface. The Fermi surface for holes is prolate along the trigonal axis and its shape is close to that of an ellipsoid of revolution. The area of the minimal principal section by the plane perpendicular to the trigonal axis is  $S_1 = (6.75 \pm 0.25) \times 10^{-42} \text{ g}^2 \text{ cm}^2 \text{ sec}^{-2}$ .<sup>2)</sup> The areas

<sup>2)</sup>All sections  $S$  will henceforth be given in  $\text{g}^2 \text{ cm}^2 \text{ sec}^{-2}$  units.

$S_2$  and  $S_3$  of the principal sections by planes perpendicular to the binary axis and the bisector practically coincide, within the limits of measurement accuracy, and are equal respectively to  $(20 \pm 1) \times 10^{-42}$  and  $(21 \pm 1) \times 10^{-42}$ . Figure 5 shows the angular dependences of the extremal sections for the case of an ellipsoid of revolution with principal sections  $S_1 = 6.75 \times 10^{-42}$  and  $S_2 = 20.0 \times 10^{-42}$  (solid curve), and a round cylinder with the same sections. It is seen from the figure that the experimental points are in better agreement with the ellipsoidal model.

The possible type of Fermi surfaces for holes have been considered in detail for the case of bismuth by Abrikosov and Fal'kovskii<sup>[21]</sup>. Figure 12 shows some types (g, f, d, b<sup>[21]</sup>) of sections of the hole surface by a plane passing through the reciprocal lattice trigonal axis. One of the main deductions of the theory of Abrikosov and Fal'kovskii is that bismuth has special directions, in which the appearance of open surfaces can be expected with increasing hole concentration. As can be seen from Fig. 12, the value of the angle  $\theta$ , which characterizes these directions can be estimated from the formula

$$\theta = S_1 \cdot 360^\circ / (S_2 \cdot 2\pi). \quad (2)$$

Substituting the values of  $S_1$  and  $S_2$ , we obtain  $\theta = 19^\circ$ . It is interesting to note that this angle agrees well with the angle  $\psi^* \approx 18^\circ$  (between the trigonal axis and the secant planes), for which

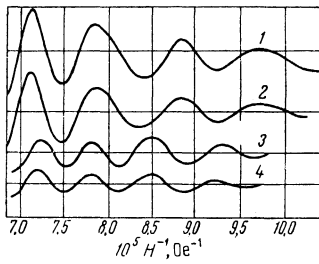
$M_i$  arb. un.


FIG. 11. High-frequency oscillations connected with the hole portion of the Fermi surface (orientation II), separated by graphic means. Curve 1— $\psi = 60^\circ$ ,  $T = 1.6^\circ\text{K}$ ; 2— $\psi = 60^\circ$ ,  $T = 2.0^\circ\text{K}$ ; 3— $\psi = 66^\circ$ ,  $T = 2.0^\circ\text{K}$ ; 4— $\psi = 66^\circ$ ,  $T = 1.6^\circ\text{K}$ .

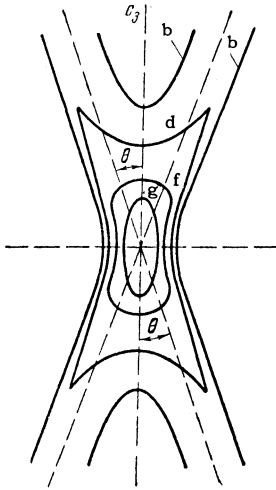


FIG. 12. Some possible types of sections of equal-energy surface for holes with the plane passing through the trigonal axis  $c_3$ , as given by [21].

splitting of the maxima and doubling of the frequency is observed. Thus, in spite of the fact that the form of the hole surface apparently differs little from variant  $g$  in [21] and is close to an ellipsoid of revolution, certain singularities appear on approaching the special directions, indicating that the dispersion deviates from quadratic for holes.

Figure 13 shows the dependence of the cyclotron effective mass on the angle  $\psi$ , calculated by the formula of I. Lifshitz [22], which is valid for an arbitrary dispersion law,

$$\frac{1}{2\pi} \frac{dS}{dE} = \frac{e\hbar}{2\pi ck} \frac{H}{(T_2 - T_1)} \ln \frac{A_1 T_2}{A_2 T_1}, \quad (3)$$

where  $A_1$  and  $A_2$  are the amplitudes of the oscillations at temperatures  $T_1$  and  $T_2$  (Fig. 11). Since the amplitude of the oscillations vanishes when  $\psi$  equals  $0^\circ$  and  $90^\circ$  the values of the effective mass in these directions are determined by extrapolation. In the quadratic approximation the hole concentration is calculated from the formula

$$n^h = \frac{2V}{(2\pi\hbar)^3} = \frac{\pi S_{av} \sqrt{S_1}}{3(\pi\hbar)^3}, \quad S_{av} = \frac{(S_2 + S_3)}{2}, \quad (4)$$

the Fermi limiting energy is

$$E_0^h = S_1/m_0 \left( \frac{dS}{dE} \right)_{\psi=0}, \quad (5)$$

and the effective masses are

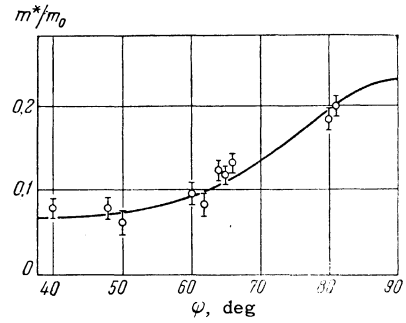


FIG. 13. Dependence of the cyclotron effective mass of the holes on the angle  $\psi$ .

$$m_1 \approx m_2 = \frac{1}{2\pi} \left( \frac{dS}{dE} \right)_{\psi=0}, \quad m_3 = m_1 \left( \frac{S_{av}}{S} \right)^2. \quad (6)$$

Thus, regardless of the dispersion law, according to the experimental data<sup>3)</sup> we have at the hole equal-energy surface

$$S_1 = (6.75 \pm 0.25)^* \cdot 10^{-42}, \quad S_2 \approx S_3 = (20.5 \pm 1)^* \cdot 10^{-42};$$

$$(dS_1/dE)/2\pi m_0 = 0.066 \pm 0.006^*,$$

$$0.068 \text{ [23]}, \quad 0.066 \text{ [24]}, \quad 0.057 \text{ [25]}.$$

In the approximation of a quadratic dispersion law<sup>4)</sup>

$$m_1/m_0 \approx m_2/m_0 = 0.066 \pm 0.006, \quad 0.057 \text{ [25]};$$

$$m_3/m_0 = 0.62 \pm 0.1^*,$$

$$0.77 \text{ [26]}; \quad m_{av}^*/m_0 = 0.14 \pm 0.015^*;$$

$$E_0^w, \text{ erg} = (1.8 \pm 0.2)^* \cdot 10^{-14}, \quad 2.4 \cdot 10^{-14} \text{ [25]};$$

$$n^w, \text{ cm}^{-3} = (2.76 \pm 0.2)^* \cdot 10^{17};$$

$$(dn/dE)_{E_0}^w, \text{ cm}^{-3} \cdot \text{erg}^{-1} = (23 \pm 3)^* \cdot 10^{30};$$

$$j^w, \text{ erg} \cdot \text{g}^{-2} \cdot \text{cm}^{-3} = 1.4 \pm 0.2^*$$

( $dn/dE$  is the density of states and  $j$  is the coefficient of electronic specific heat).

2. Electronic part of the Fermi surface. From Figs. 4–6 it follows that the form of the Fermi surface for the electrons agrees qualitatively with the Jones-Shoenberg model.

Let us place the origin at the center of the surface and denote the axis along the binary axis by  $p_1$ , in the direction of the elongation by  $p_2$ , and in a perpendicular direction by  $p_3$ . The volume and the form of the electron surface are determined by the three principal cross sections  $S_1$

<sup>3)</sup>The asterisk denotes the results of the present work.

<sup>4)</sup>The parameters of the electrons and holes as given by the Abrikosov and Fal'kovskii theory [21] are not calculated because the constants in the equation of [21] are presently still being computed.

(for  $p_2 = 0$ ),  $S_2$  (for  $p_3 = 0$ ), and  $S_3$  (for  $p_1 = 0$ ), and by the character of the angular dependence of its extremal sections as the direction of the magnetic field is varied in the planes  $(p_1, p_2)$  and  $(p_2, p_3)$ . In the first case this dependence is close to ellipsoidal (Fig. 6). The sections  $S_1$  and  $S_3$  correspond to  $\psi = -84^\circ$  in Fig. 4 and 0 and  $60^\circ$  in Fig. 6, and can be determined sufficiently accurately without any special assumption concerning the forms of the surfaces:

$$S_1 = (1.34 \pm 0.05) \cdot 10^{-42}, \quad S_3 = (22 \pm 1) \cdot 10^{-42}.$$

Difficulties arise in the determination of the section  $S_2$ , because the oscillation pattern is quite complicated near  $\psi = 6^\circ$  (Fig. 4) and extrapolation based on the ellipsoidal model does not lead to results that agree with the experimental data for the intermediate sections of the "ellipsoid" of the Fermi surface when the ellipsoid has a different orientation in p-space. Extrapolation of sections c-d and b-g of Fig. 4 leads to  $S_2 = 15 \times 10^{-42}$  and  $\xi = 7^\circ$ . The curves of the angular dependence of  $S_m$ , plotted for ellipsoids with the same parameters, are designated in Figs. 4 and 5 by 1', 2', and 3'. In Fig. 4 the curves 2' and 3' deviate noticeably from the experimental points in the angle region  $155-160^\circ$ . On the other hand, if we use for the extrapolation the values of  $S_m$  in the same region of angles, then  $S_2 \approx 13 \times 10^{-42}$  and  $\xi = 6^\circ$ . The corresponding curves of the angular dependence of  $S_m$  are numbered 1, 2, and 3 on Figs. 4 and 5. We see that curve 1 of Fig. 4 passes below the experimental points for  $9^\circ < \psi < 13^\circ$ . It is possible that the difficulties in reconciling the experimental data with the ellipsoidal model are connected with the deviation of the shape of the Fermi surface from a triaxial ellipsoid, which is manifest in the region of the sections close to  $S_2$ .

The singularities of the Fermi surface in the region of large sections are also manifest by the following two circumstances: the frequency doubling observed for sections passing through the reciprocal lattice trigonal axis at an angle  $\psi^* = 2.8-3^\circ$  to the  $p_2$  axis (Fig. 10), and the absence of noticeable oscillations of the fundamental frequency corresponding to the "ellipsoid" 1 of Fig. 4 at angles  $1^\circ < \psi < 9^\circ$ . From the point of view of the ellipsoidal model it is not clear why oscillations are observed for orientation III at practically all values of  $\psi$  (up to sections  $S \approx 22 \times 10^{-42}$ ), while for orientation I the main oscillations disappear abruptly (on approaching the angle  $6^\circ$ ) at values of  $\psi$  equal to 1 and  $9^\circ$ , although in the latter case they should correspond to sections  $S_m \ll 22 \times 10^{-42}$ .

The data given in Figs. 6 and 10 agree well with the notion that the plane passing through the axis  $p_2$  and  $p_3$  is a symmetry plane for each "ellipsoid." However, the difference in the character of the oscillations to the right and to the left of the angle  $\psi = 6^\circ$  (Fig. 4) indicates apparently that the plane passing through  $p_1$  and  $p_3$  is not a symmetry plane. In particular, the unilateral bending of the Fermi surface, which follows from the theory of Abrikosov and Fal'kovskii<sup>[21]</sup>, may occur.

We have pointed out that the theory of Abrikosov and Fal'kovskii predicts the existence of special directions, in which open cross sections can occur with increasing hole concentration. If we assume that for electrons the pattern of occurrence of such directions is similar to that for holes (Fig. 12), then the corresponding angle  $\theta$  estimated by formula (2) for sections passing through the  $p_2$  axis,  $\theta \approx 3^\circ$ , agrees well with the angle  $\psi^* = 2.8-3^\circ$ . Thus, frequency doubling occurs on approaching the singular directions in the reciprocal lattice of bismuth for the case of electrons, too.

In estimating the main parameters of the electronic part of the Fermi surface, we confine ourselves to an examination of the ellipsoidal approximation with non-quadratic dispersion in the theory of Cohen<sup>[27]</sup>, who takes account of the dependence of the effective mass on the energy, as confirmed by Weiner<sup>[7]</sup> and Smith<sup>[25]</sup>. We assume that  $S_2 = (14 \pm 1.5) \times 10^{-42}$ . The low-frequency oscillations at  $\psi = 1.5-3^\circ$  and  $\psi = 7-9^\circ$  must then be regarded as the result of the frequency doubling, and the oscillations in the interval  $3-7^\circ$  as the third harmonic of the "ellipsoids" 2 and 3 of Fig. 4. The vanishing of the fundamental oscillations from the "ellipsoids" 1 at angles  $1^\circ < \psi < 9^\circ$  can be attributed within the framework of the ellipsoidal model to a superposition of the second harmonic from the coinciding "ellipsoids" 2 and 3, shifted in phase by  $\pi/2$ . The extinction of the second harmonic near  $\psi = 6^\circ$  may also be the factor favoring the appearance of the third harmonic in this angle region.

Data on the electronic equal-energy surface can be divided into those independent of the dispersion law (A) and those dependent on the specifically assumed dispersion law (B).

#### A. Experimental data:

$$S_1 = (1.34 \pm 0.05) \cdot 10^{-42}, \quad 1.37 \cdot 10^{-42} \text{ [24]}, \quad 1.35 \cdot 10^{-42} \text{ [28]};$$

$$S_3 = (22 \pm 1) \cdot 10^{-42};$$

$$(dS_1/dE)/2\pi m_0 = 0.0084 \pm 0.001^*, \quad 0.0092 \text{ [24]};$$

$$\xi = 6^\circ \pm 0.3^*, \quad 6^\circ \pm 15' \text{ [24]}.$$

## B. Calculated data:

$$S_2 = (14 \pm 1.5) \cdot 10^{-42}.$$

Effective masses in the coordinate system fixed in the ellipsoids:

$$m'_1/m_0 = 0.0052 \pm 0.0012^*, 0.0088 [^{23}], 0.0062 [^{25}];$$

$$m'_2/m_0 = 1.5 \pm 0.3^*, 1.8 [^{23}], 1.3 [^{25}];$$

$$m'_3/m_0 = 0.013 \pm 0.003^*, 0.009 [^{23}], 0.01 [^{25}];$$

$$m_{av}/m_0 = 0.047 \pm 0.01^*.$$

Cyclotron masses:

$$\sqrt{m'_2 m'_3}/m_0 = 0.14 \pm 0.03^*, 0.13 [^{24}];$$

$$\sqrt{m'_1 m'_2}/m_0 = 0.09 \pm 0.02^*.$$

Effective masses in the coordinate system fixed in the crystal lattice:

$$m_1/m_0 = 0.0052 \pm 0.0012^*, 0.0088 [^{23}], 0.0062 [^{25}];$$

$$m_2/m_0 = 1.5 \pm 0.3^*, 1.8 [^{23}], 1.30 [^{25}];$$

$$m_3/m_0 = 0.03 \pm 0.006^*, 0.023 [^{23}], 0.017 [^{25}];$$

$$m_4/m_0 = \pm 0.16^*, \pm 0.16 [^{23}], -0.085 [^{25}].$$

For the ellipsoidal model with non-quadratic dispersion law<sup>[27]</sup> we have

$$E_0^e, \text{ erg} = (3.7 \pm 0.2) \cdot 10^{-14}, 4 \cdot 10^{-14} [^{25}];$$

and for a quadratic dispersion law

$$E_0^e, \text{ erg} = (2.8 \pm 0.1) \cdot 10^{-14}, (2.5 \pm 0.1) \cdot 10^{-14} [^{24}].$$

The electron concentration per ellipsoid

$$n^e, \text{ cm}^{-3} = (1.0 \pm 0.1) \cdot 10^{17}, 0.8 \cdot 10^{17} [^{25}];$$

$$(dn/dE)_{E_0}^e, \text{ cm}^{-3} \cdot \text{erg}^{-1} = (18 \pm 2) \cdot 10^{30};$$

$$j^e, \text{ erg} \cdot \text{g}^{-2} \cdot \text{cm}^{-3} = 1.1 \pm 0.2^*.$$

3. Singularities of the oscillations. As noted above, for the electrons (orientation III) in the angle region  $\psi^* = \pm 3^\circ$ , and for holes (orientations I and II) in the angle region  $\psi^* = 72^\circ$  and  $\psi^* = 108^\circ$ , the maxima of the oscillations are split and this leads to the vanishing of the fundamental frequency and the appearance of a doubled frequency at these angles. If we interpret this phenomenon as a superposition of a high frequency component on the fundamental frequency, then we must assume that for angles  $68^\circ < \psi < 78^\circ$ ,  $102^\circ < \psi < 112^\circ$  and  $1^\circ < \psi < 4^\circ$ ,  $-4^\circ < \psi < -1^\circ$  we observe simultaneously the cross sections of two different surfaces, an event of low probability. It is likewise hardly probable that this phenomenon is connected with the sharp increase in the second harmonic, since the corresponding fundamental frequency vanishes near the angles  $\psi^* = 72^\circ$ ,  $\psi^* = 108^\circ$ , and  $\psi^* = \pm 3^\circ$ .

It is possible that the observed phenomenon is connected with the change in the value of spin splitting of the energy levels. Gold<sup>[26]</sup> has shown that the strong spin-orbit interaction<sup>[27]</sup> in bismuth

causes the Landau levels to be split by an amount equal to the distance  $\Delta E$  between the levels. Since the angles  $\psi^*$  are in good agreement with the special directions  $\theta$  in the theory of<sup>[21]</sup>, it is quite probable that on approaching these directions the value of the spin splitting decreases and becomes equal to  $\Delta E/2$  at the angles  $\psi^*$ , causing doubling of the frequency. The large spin splitting of the energy levels apparently also explains the discrepancy between the theoretical ( $\pi/4$ ) and experimental ( $-\pi \pm \pi/4$ ) values of the oscillation phases in the Landau formula, a discrepancy noted in<sup>[4,5]</sup>. It is likewise not excluded that this effect can be connected with singularities of the energy spectrum of the electrons, considered in<sup>[21]</sup>.

Another feature of the oscillations, manifest in the dependence of the frequency on the intensity of the inverse magnetic field, can be caused by the following factors.

a) Change in the mutual orientation of the crystal lattice of the specimen in the direction of the magnetic field with increase in the latter, if the phase of the oscillations depends strongly on the angle  $\psi$ . We note that in this case the main cause of the change in frequency is not the transition to larger or smaller sections of the Fermi surface as a result of the change in the angle  $\psi$ , but precisely the strong angular dependence of the oscillation phase at a fixed field  $H$ . Variations of  $\psi$  during the measurements are determined by the error angle  $\Delta\psi_1$  of the servomechanism, the torsion angle  $\Delta\psi_2$  of the rod, and the angle  $\Delta\psi_3$  connected with the rotation of the induction  $\mathbf{B} = \mathbf{H} + 4\pi\mathbf{I}$  in the specimen due to the periodically varying magnetization  $\mathbf{I}$ . Special experiments, in which  $\Delta\psi_1$  and  $\Delta\psi_2$  were decreased to approximately one-tenth from  $\sim 1'$ , did not lead to a noticeable increase in the dependence of the frequency on  $1/H$ . The value of  $\Delta\psi_3$  was determined by the ratio  $|4\pi\mathbf{I}|/H$ , and is close to  $1'$  in the case of bismuth. The angle  $\Delta\psi_3$  determines the limit to which the variations of the angle  $\psi$  can be decreased. We note that if the "phase shift" effect does take place in spite of the smallness of the variation of  $\psi$ , then the true frequency determining  $S_m$  is the frequency averaged over several high-frequency periods. This averaging is best carried out in the region of the weakest magnetic fields, since the "phase shift" effect increases with increasing  $H$ , owing to the increase in the derivative  $\partial\psi/\partial H$ .

b) Beats resulting from a superposition of two nearly equal frequencies, for example the fundamental frequency connected with the large cross sections  $S_m$ , and the  $p$ -th harmonic of smaller cross sections. To clarify this question it is necessary to trace the dependence of the frequency

and amplitude of oscillations on  $1/H$  over a sufficiently broad interval of fields, which is impossible in the majority of cases.

c) Deviation of the dispersion law from quadratic. Since the deviation from the quadratic dispersion law should appear most strongly in the large sections, for which the oscillations are observed only in strong fields, we do not have sufficient data to be able to state which of the three foregoing mechanisms is decisive.

4. Some remarks on the general character of the bismuth energy spectrum. Bismuth is a metal with an equal number of electrons and holes. This requirement is satisfied by a model consisting of one hole surface and three electronic surfaces. In many investigations, for example<sup>[7,29-31]</sup>, the large value of the coefficient  $j$  of the electronic specific heat is explained by assuming the existence in bismuth of a group of heavy holes with end-point energy fluctuating between 7 and 30°K. Recently Lerner<sup>[31]</sup> reported the observation in bismuth of a group of heavy holes with concentration  $1.7 \times 10^{17} \text{ cm}^{-3}$  and a group of heavy electrons with concentration  $1.3 \times 10^{17} \text{ cm}^{-3}$ . However, the data given by Lerner are, from our point of view, not sufficiently convincing, since the high-frequency oscillations which he ascribes to groups of heavy carriers could be caused by other factors. Consequently at present we can speak with sufficient reliability only of the group of electrons and the group of holes, which in accordance with the theory of Abrikosov and Fal'kovskii<sup>[21]</sup> presupposes the existence in bismuth of one hole and three electronic surfaces. Here, however, difficulties remain in reconciling this model (for a quadratic dispersion law) with the data on the electronic specific heat. For such a reconciliation it is necessary that the density of the states on the Fermi boundary exceed by 3-4 times the electron and light-hole state density that follows from the quadratic dispersion law.

<sup>1</sup> Brandt, Dubrovskaya, and Kytin, JETP 37, 572 (1959), Soviet Phys. JETP 10, 405 (1960).

<sup>2</sup> N. B. Brandt, PTÉ No. 2, 1960.

<sup>3</sup> N. B. Brandt, JETP 38, 1355 (1960), Soviet Phys. JETP 11, 975 (1960).

<sup>4</sup> D. Shoenberg, Proc. Roy. Soc. 170, 341 (1939).

<sup>5</sup> J. S. Dhillon and D. Shoenberg, Phil. Trans. Roy. Soc. (London) A248, 1 (1955).

<sup>6</sup> N. B. Brandt and M. V. Razumeenko, JETP 39, 276 (1960), Soviet Phys. JETP 12, 198 (1961).

<sup>7</sup> D. Weiner, Phys. Rev. 125, 1226 (1962).

<sup>8</sup> P. B. Alers and R. T. Webber, Phys. Rev. 91, 1060 (1953).

<sup>9</sup> Reynolds, Hemstreet, Leinhardt, and Triantos, Phys. Rev. 96, 1203 (1954).

<sup>10</sup> M. C. Steele and J. Babiskin, Phys. Rev. 98, 357 (1955).

<sup>11</sup> W. C. Overton and T. G. Berlincourt, Phys. Rev. 99, 1165 (1955).

<sup>12</sup> J. Babiskin, Phys. Rev. 107, 981 (1957).

<sup>13</sup> R. A. Connell and J. A. Marcus, Phys. Rev. 107, 940 (1957).

<sup>14</sup> D. H. Reneker, Phys. Rev. 115, 303 (1959).

<sup>15</sup> W. S. Boyle and K. F. Rodgers, Phys. Rev. Lett. 2, 338 (1959).

<sup>16</sup> Boyle, Hsu, and Kunzler, Phys. Rev. Lett. 4, 278 (1960).

<sup>17</sup> G. E. Smith, Phys. Rev. 115, 1561 (1959).

<sup>18</sup> N. B. Brandt and Ya. G. Ponomarev, PTÉ No. 6, 114 (1961).

<sup>19</sup> P. L. Kapitza, Proc. Roy. Soc. A119, 358 (1928).

<sup>20</sup> K. A. Velikzhanina and S. N. Rzhevkin, ZhTF 17, No. 12.

<sup>21</sup> A. A. Abrikosov and L. A. Fal'kovskii, JETP 43, 1089 (1962), Soviet Phys. JETP 16, 769 (1963).

<sup>22</sup> I. M. Lifshitz and A. M. Kosevich, DAN SSSR 96, 963 (1954); JETP 29, 730 (1955), Soviet Phys. JETP 2, 636 (1956).

<sup>23</sup> Galt, Yager, Merritt, Cetlin, and Brailsford, Phys. Rev. 114, 1396 (1959).

<sup>24</sup> Khaikin, Mina, and Édel'man, JETP 43, 2063 (1962), Soviet Phys. JETP 16, 1459 (1953).

<sup>25</sup> G. E. Smith, Phys. Rev. Lett. 9, 487 (1962).

<sup>26</sup> Smith, Galt, and Merritt, Phys. Rev. Lett. 4, 276 (1960).

<sup>27</sup> M. H. Cohen and E. I. Blount, Phil. Mag. 5, 115 (1960); Phys. Rev. 121, 387 (1961).

<sup>28</sup> E. P. Vol'skii, JETP 43, 1123 (1962), Soviet Phys. JETP 16, 793 (1963).

<sup>29</sup> V. Heine, Proc. Phys. Soc. A69, 513 (1956).

<sup>30</sup> A. L. Jain and S. H. Koenig, Phys. Rev. 127, 442 (1962).

<sup>31</sup> L. S. Lerner, Phys. Rev. 127, 1480 (1962); 130, 605 (1963).

Translated by J. G. Adashko